Journal of Petroleum Exploration and Production Technology (2021) 11:2327–2345
https://doi.org/10.1007/s13202-021-01192-4

ORIGINAL PAPER-EXPLORATION GEOLOGY

CO_2 storage capacity estimation under geological uncertainty using 3-D geological modeling of unconventional reservoir rocks in Shahejie Formation, block Nv32, China

Ayman Mutahar AlRassas[1] · Shaoran Ren[1] · Renyuan Sun[1] · Hung Vo Thanh[2] · Zhenliang Guan[3]

Received: 24 March 2021 / Accepted: 16 May 2021 / Published online: 2 June 2021

Abstract

Underground CO_2 storage is a promising technology for mitigating climate change. In this vein, the subsurface condition was inherited a lot of uncertainties that prevent the success of the CO_2 storage project. Therefore, this study aims to build the 3D model under geological uncertainties for enhancing CO_2 storage capacity in the Shahejie Formation (Es1), Nv32 block, China. The well logs, seismic data, and geological data were used for the construction of 3-D petrophysical models. The target study area model focused on four units (Es1 × 1, Es1 × 2, Es1 × 3, and Es1 × 4) in the Shahejie Formation. Well logs were utilized to predict petrophysical properties; the lithofacies indicated that the Shahejie Formation units are sandstone, shale, and limestone. Also, the petrophysical interpretation demonstrated that the *Es*1 reservoir exhibited high percentage porosity, permeability, and medium to high net-to-gross ratios. The static model showed that there are lateral heterogeneities in the reservoir properties and lithofacies; optimal reservoir rocks exist in Es1 × 4, Es1 × 3, and Es1 × 2 units. Moreover, the pore volume of the Es1 unit was estimated from petrophysical property models, ranging between 0.554369 and 10.03771×10^6 sm^3, with a total volumetric value of 20.0819×10^6 sm^3 for the four reservoir units. Then, the 100–400 realizations were generated for the pore volume uncertainties assessment. In consequence, 200 realizations were determined as an optimal solution for capturing geological uncertainties. The estimation of CO_2 storage capacity in the Es1 formation ranged from 15.6 to 207.9×10^9 t. This result suggests the potential of CO_2 geological storage in the Shahejie Formation, China.

Keywords 3-D geological model · Geological uncertainty · CO_2 storage capacity · Unconventional oil reservoir · Tight oil reservoir · Nv32 block

Introduction

Carbon capture and storage is an alternative approach for minimizing CO_2 emissions to the atmosphere (Vo Thanh et al. 2019; Ampomah et al. 2017b). In general, CO_2 can be stored in different subsurface sites, such as deep saline aquifers, coal bed seams, unconventional resources, and depleted petroleum reservoirs (Vo Thanh et al. 2020b, 2020a). Among these storage sites, saline aquifers have the largest CO_2 storage capacity (Vo Thanh et al. 2019). However, depleted petroleum reservoirs are the most suitable candidates because the CO_2 injection process can improve oil recovery (Vo Thanh et al. 2019). Improving the oil recovery is therefore feasible by injecting CO_2 into oil-bearing reservoirs. This method, known as CO_2-enhanced oil recovery (CO_2-EOR), combined with gas storage, can be used to alleviate the cost of sequestration (Zhong and Carr 2019; Vo Thanh et al. 2019).

Mitigating CO_2 seepage hazards implies a reduction in perpendicular CO_2 migration by selecting appropriate storage sites. Three-dimensional (3-D) reservoir geological modeling is currently an effective method for evaluating the CO_2 storage capacity. Several recent studies have examined the CO_2 storage capacity using 3-D geological

✉ Ayman Mutahar AlRassas
alrassas1989@gmail.com

✉ Hung Vo Thanh
vothanhhung198090@gmail.com

[1] School of Petroleum Engineering, China University of Petroleum (East China), Qingdao, China

[2] School of Earth and Environmental Sciences, Seoul National University, Seoul, Korea

[3] Faculty of Earth Resources, China University of Geosciences, Wuhan, China

models (Ampomah et al. 2017a; Anderson 2017; Spencer 1987; Alcalde et al. 2018). These models are an appropriate approach that integrates all available geological, geophysical, and engineering data (Hirsche et al. 1997; Bueno et al. 2011; Abdideh and Bargahi 2012; Dai et al. 2016). According to recent studies, 3-D geostatistical modeling can support the evaluation of potential CO_2 storage areas in hydrocarbon reservoirs (Vo Thanh et al. 2019, 2020b; Rahim et al. 2015; Yin et al. 2017). Therefore, geological modeling is a promising tool for maximizing CO_2 utilization in petroleum resources (Kamali et al. 2013; Zamora Valcarce et al. 2006; Metwalli et al. 2017).

The assessment and management of subsurface uncertainties have increasingly become more important in the petroleum industry sector. The aim is to enhance reserve portfolios, implement appropriate field developments, and strengthen technical operations, particularly with respect to well planning (Kamali et al. 2013). Stochastic approaches are used to screen and value hydrocarbon assets (Bueno et al. 2011; Kamali et al. 2013).

Using Monte Carlo simulations, subsurface models can reduce the geological uncertainty, thus improving the probability of CO_2 storage project success (Dai et al. 2016; Hirsche et al. 1997). Additionally, the geological uncertainty assessment provides a better understanding of the P10, P50, and P90 values. These values can provide an enhanced perspective on the static and dynamic CO_2 storage capacity at the target site (Bueno et al. 2011).

As sampling and direct multiplication of Monte Carlo loops is straightforward and fast, thousands of Monte Carlo loops can be implemented for accurate output distributions. Although these methods are fast, determining the intrinsic dependencies among all of the input variables is difficult, often providing no quantification or visualization of the spatial location and variability in the uncertainty. A 3-D model is an alternative approach for volumetric determinations, facilitating a practical treatment of the dependence between various input variables while enhancing knowledge on the spatial heterogeneity in the uncertainty (Kamali et al. 2013; Abdideh and Bargahi 2012; Kamali et al. 2013). The geological structure of a reservoir, variation in its petrophysical properties, and the gas oil contact and oil water contact are considered the main sources of uncertainty (Kamali et al. 2013). The probabilistic distribution of the gross rock volume (GRV) (MMm^3) and stock-tank oil initially in place (STOIIP) can then be determined, as well as the use of reliable volume computations and risk evaluations (Bueno et al. 2011; Satter and Iqbal 2016). Moreover, few studies have focused on the gap between CO_2 storage and geological uncertainties, whereas the performance of the CO_2 storage assessment affects the geological uncertainty. Therefore, we address comprehensive 3-D reservoir geological modeling as a multi-objective function of the four reservoir units in the Paleogene Shahejie Formation (Es1) and compute the CO_2 storage capacity based on the geological uncertainty in the Nv32 block of the Shenvsi oilfield (Fig. 1). This study also aims to provide a systematic overview of the potential for the geological sequestration of CO_2 while improving oil recovery and CO_2 storage.

Study area

The Shahejie Formation (Es1) of the Nv32 block is situated in the Shenvsi oilfield in the southern region of Cangzhou City, Hebei Province. The Shenvsi oilfield structure is located within the Cangxian and Kongdian structures. Several oilfields exist as a result of the structural complexity and fault evolution within the Shenvsi oilfield. Furthermore, the sedimentary stratigraphy of the study area comprises

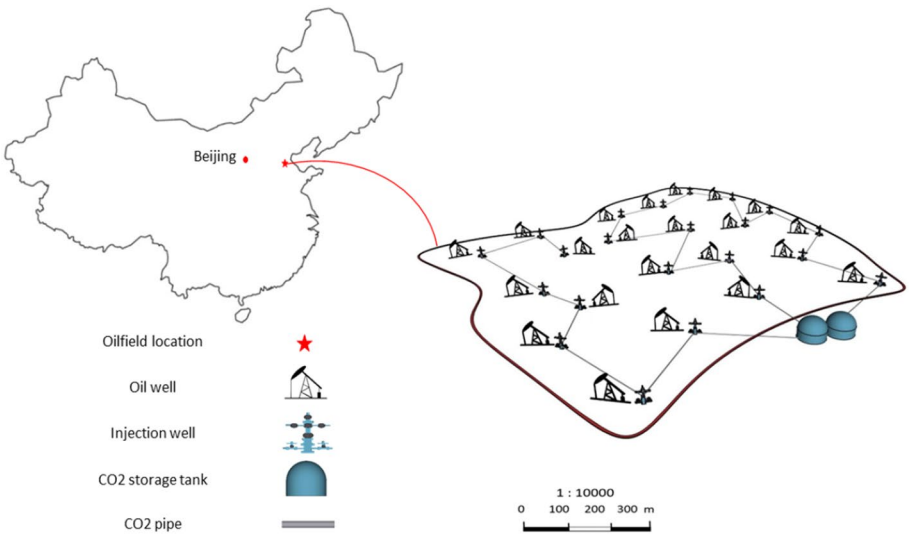

Fig. 1 Map of the Shahejie Formation in the Nv32 block

Eocene to Pliocene rock successions, which include four major lithostratigraphic formations, i.e., the Shahejie, Dongying, Guantao, and Minghuazhen formations, from oldest to youngest. The structural area of the sand–oil top structure is 2.0 km^2, the structural width is 100 m, the proven oil-bearing area is 1.4 km^2, and the petroleum geological reserves are 225×10^4 t (Rassas et al. 2020; Ling and Qingkui 2017). Figure 1 shows the oilfield locations.

Databases and methodology

Figure 2 presents the workflow and databases used in this study, including the check-shot data, 3-D seismic volume, lithological characteristics, geological reports, deviation data, and wireline logs [consisting of the spontaneous potential (SP), gamma-ray (GR), caliper (CAL), and acoustic impedance (AC)] from the 22 available drilled wells in block Nv32, Shenvsi oilfield. These geophysical and geological data were used to quantify and improve the accuracy of the internal structure of the reservoir and the petrophysics of its heterogeneity. These data were incorporated into the Petrel software and utilized to build 3-D geological static models, such as structural, lithofacies, and petrophysical property models, as well as to calculate the volume of the reservoir. Uncertainty analysis of the constructed reservoir geological models was performed to compute the CO_2 storage capacity. Additionally, the theoretical CO_2 sequestration capacity was established based on a specific formulation introduced by previous studies (Bradshaw et al. 2007; Mckee 2005; Pingping et al. 2009).

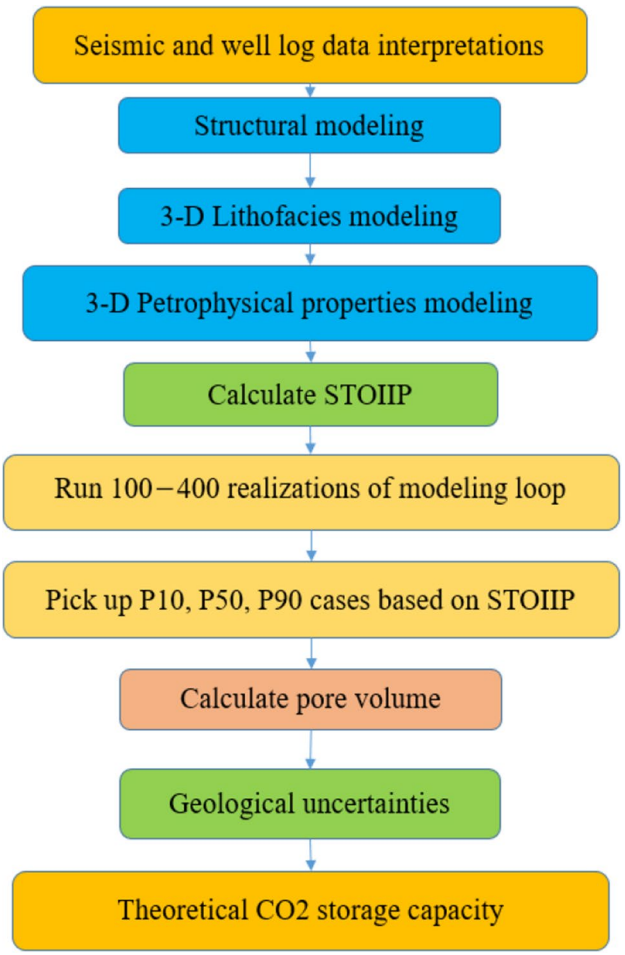

Fig. 2 Workflow used in this study

Reservoir modeling

The 3-D geological model was built using the Petrel software to show the structural features of block Nv32, the vertical and horizontal distributions of the petrophysical properties (i.e., the porosity and permeability), and the lithofacies of the Es1 formation units in the Shenvsi oilfield.

Structural modeling

Structural modeling is the major stage in constructing a 3-D geological model (Abdel-Fattah et al. 2018; Agyare Godwill and Waburoko 2016; Jika et al. 2020). The model of the structural features in block Nv32 was constructed using interpretations of the 3-D seismic data. The seismic data show that the Shenvsi oilfield, including block Nv32, primarily comprises horsts and tilted fault blocks (Fig. 3).

This structural style indicates that the Shenvsi oilfield can be classified as a rifting basin. The 3-D seismic interpretation data, including the reservoir surface tops and measured fault surfaces, were imported into the Petrel software to build the structural model.

The first stage of building a structural model was the selection of structural faults based on the 3-D seismic data (Fig. 3). The fault surfaces were constructed by employing the fault polygon in Petrel for each type of vertical fault, diagonal fault, curving fault, and faults with various geometrical structures, each congruous to its polygon. The primary surface was defined by implementing fault polygons with varying stratification planes (Fig. 4a and b). Subsequently, the structural domain of the reservoir rock horizons was selected from the 3-D seismic data and then converted from a time version to a depth version. Finally, the skeleton of the structural model was realized by associating the 3-D fault surfaces with the reservoir rock horizons of the Es1 formation (Fig. 4c).

Lithofacies modeling

The lithofacies model of block Nv32 was constructed based on the lithofacies interpretation of the sedimentary

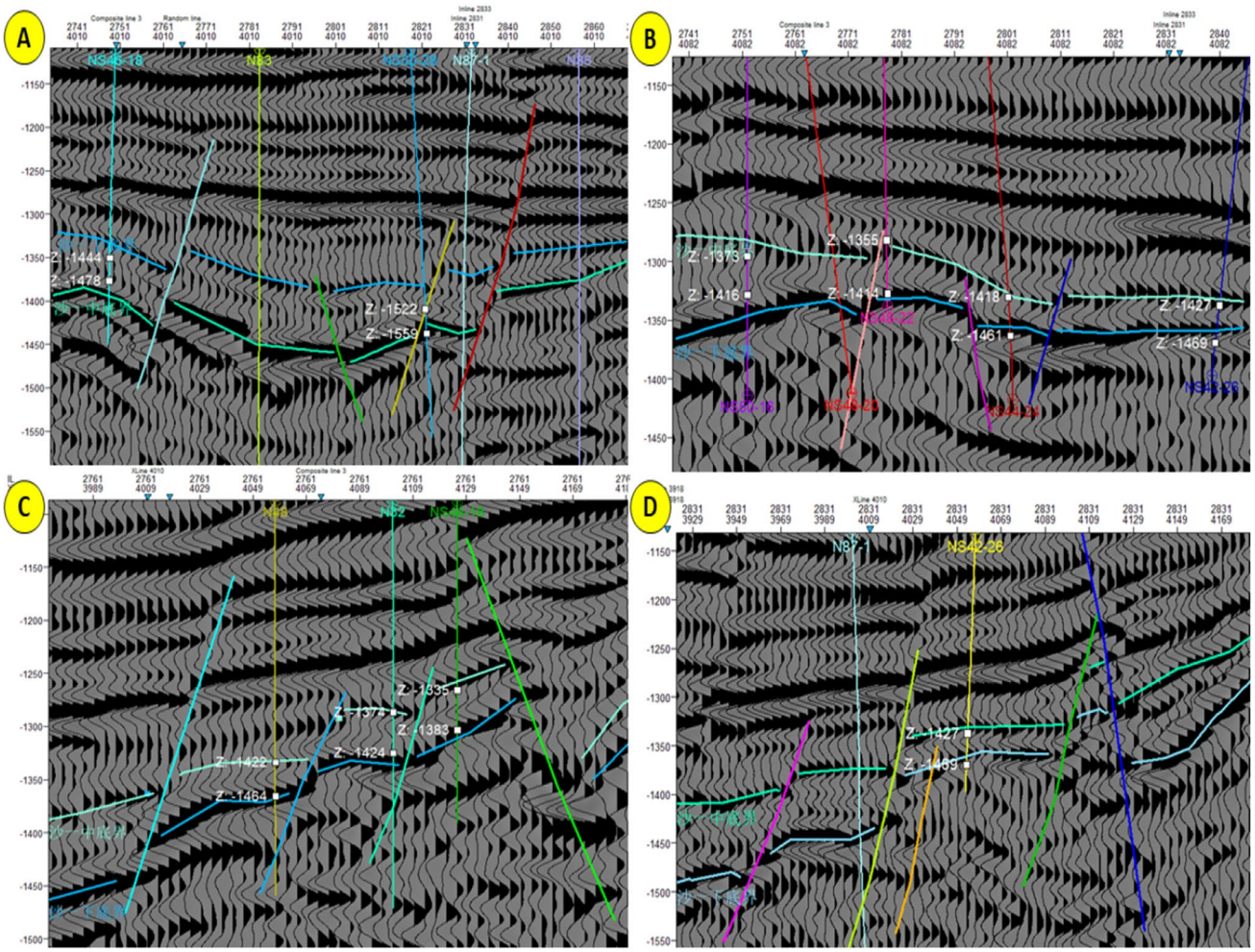

Fig. 3 Seismic sections showing the reservoir tops of the Formation units associated with normal faults **a**. Es1×1, **b**. Es1×2, **c**. Es1×3, and **d**. Es1×4. Vertical lines represent the locations of the wells

environments obtained from the well logs. The well log-based lithofacies results showed that the Es1 units in block Nv32 mainly comprise three lithologies, i.e., shale, limestone, and sandstone. The well log-based lithofacies results from the 22 wells were imported to the Geomap 3.6 software. Additionally, data for the facies model were then extracted from Geomap 3.6 and imported to the Petrel software to construct the lithofacies model of block Nv32.

Facies modeling requires different facies approaches, such as object modeling, which is typically utilized for lithofacies modeling. However, in this model, the assigned values were employed to populate discrete lithofacies models based on grids of different bodies with various geometries, facies codes, and fractions. Facies modeling in a 3-D space was simulated using the simulation sequential indicator (SIS) method.

Petrophysical property modeling

Petrophysical property modeling is a critical stage in reservoir characterization because it significantly influences the heterogeneity and flows modeling. In this study, the petrophysical properties of the four formation units within the Es1 Formation of block Nv32 were estimated from the well-logging data using the Petrel software. Based on the well log, the petrophysical properties were up-scaled and laterally dispersed using the sequential Gaussian simulation (SGS) method. This method is the most prominent geostatistical technique for constructing stochastic random fields of continuous parameters, including permeability and porosity (Pyrcz and Deutsch 2014; Zhong and Carr 2019). The SGS method has been successfully implemented to generate several equiprobable realizations of the distributions of the petrophysical properties to obtain the uncertainty (Mckee 2005; Pingping et al. 2009).

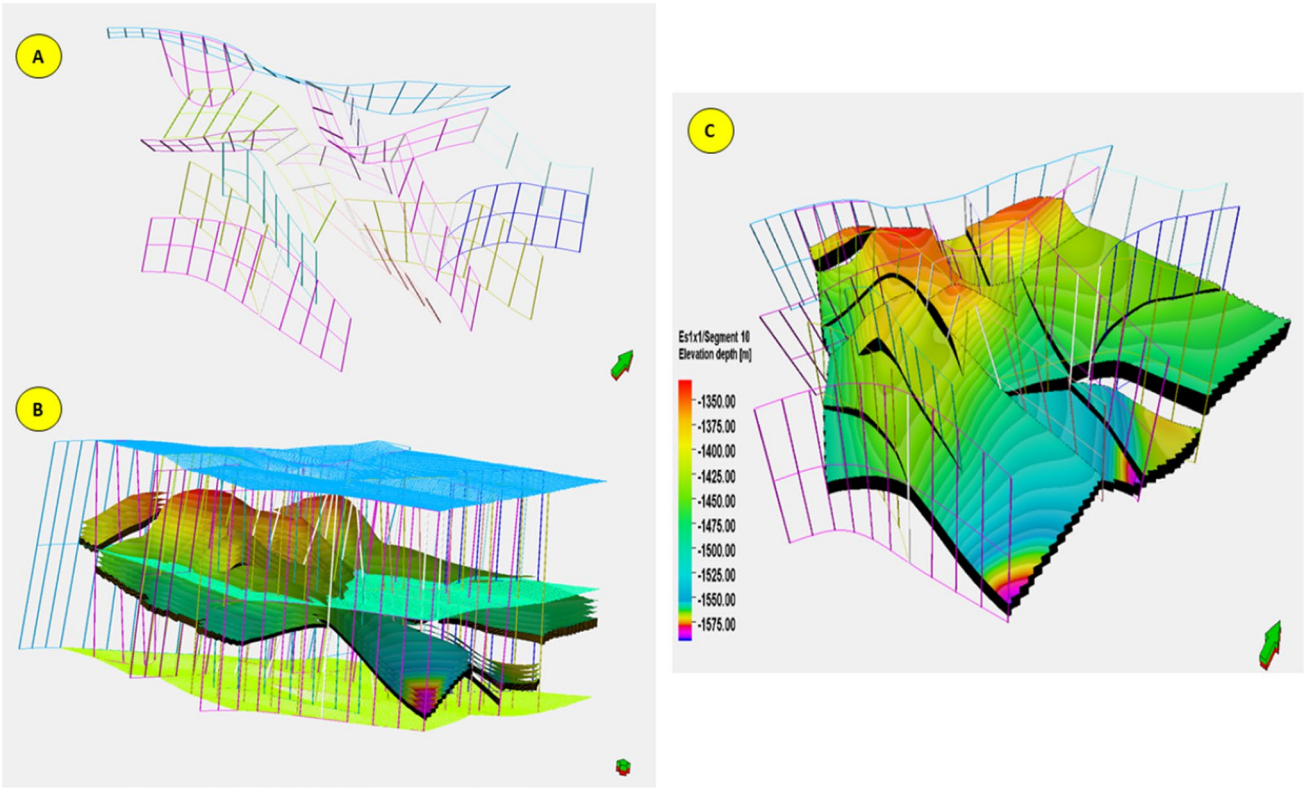

Fig. 4 Structural model of block Nv32. **a**. Fault pillars and polygons as a structural framework. **b**. Fault pillars associated with the reservoir horizons. **c**. Reservoir horizons (Es1 × 1–Es1 × 4), along with the interpreted faults

Furthermore, this algorithm is more effective than a truncated simulation because it does not consider the orderly transformation between facies types (Al-Mudhafar 2018). Previous studies provide a more detailed description of the methodology for the SGS (Pyrcz and Deutsch 2014; Zhong and Carr 2019).

Volumetric analysis

Volumetric analysis of the reservoir rock allows the calculation of the volume of hydrocarbon in the reservoir. The determination of the reservoir rock volume is commonly an important calculation because it serves as a reference for the exploration and development of oil and gas fields. In this study, the reserves, in terms of the STOIIP in the Shahejie Formation, were determined after the 3-D reservoir model was completed, including the structural and petrophysical property models. Moreover, the STOIIP in the Shahejie Formation was estimated as follows (Satter and Iqbal 2016):

$$\mathrm{STOIIP} = 7758 \times A \times h \times \phi \times \left(1 - S_W\right) \times \frac{1}{B_o}, \quad (1)$$

where A = reservoir area (acres); h = reservoir thickness (ft); Sw = water saturation (fraction); Bo = formation volume factor (bbl/stb).

Uncertainty analysis

The construction of a geological reservoir model requires a significant quantity of data to reduce the associated uncertainties. Thus, understanding the uncertainty associated with reservoir geological modeling as a support for oil industry decisions is essential. An awareness of uncertainty management based on forecasting hydrocarbon volumes has increased in recent decades as a consequence of accurate 3-D geological models constructed using advanced technologies. Many studies have addressed the uncertainties inherent in geological modeling. (Lelliott et al. 2009) classified the sources of uncertainties associated with geological modeling into data density (the borehole density was employed to build the model), data quality (quality of the model data, including the logging quality, sample type, borehole attitude, and drilling approach), geological complexity (geological heterogeneity across the site), and software modeling. In reservoir engineering, as stated by (Zabalza-Mezghani et al. 2004), the sources of uncertainty can be categorized

throughout the geological modeling process. These uncertainties occur in static geological models, fluid flow modeling, up-scaling, the incorporation of production data, and economic assessments. Bueno et al. (2011) categorized the various uncertainty behaviors, including discrete and deterministic stochastic uncertainties. Therefore, the uncertainties associated with the input datasets utilized to construct 3-D geological models cannot be represented by a single deterministic realization, which produces significant uncertainty during reservoir estimation when combining sources.

Furthermore, 3-D models still comply with these rules, and the presence of significant uncertainty elements, which occur in model construction, remains irrefutable. The volumetric equation is usually used to define the number of errors; however, modern technology has enabled the use of 3-D models as a basis to facilitate evaluations of this uncertainty within a reservoir. The use of these 3-D models has several benefits over an assessment, depending on the direct implementation of volumetric equations. Among these benefits, 3-D models facilitate the realistic visualization of intrinsic correlations; the resulting accuracy of the uncertainty estimation allows the establishment of a strong foundation for capital management. In this model, for the geological uncertainty, calculating the pore volume is essential. Thus, 100–400 cases were simulated for the uncertainty evaluation to define the pore volume by changing the variogram parameter in the Petrel software. The probability distribution of the pore volume was determined using the Monte Carlo sampling approach. Subsequently, the results for P10, P50, and P90 were adopted for the risk evaluation of the theoretical CO_2 storage capacity.

Theoretical CO_2 Storage Capacity

This study mainly focused on the theoretical CO_2 storage capacity in the structural and stratigraphic trapping, given as follows:

$$M_{CO2} = A \times h \times \phi \times \left(1 - S_{wiir}\right) \times B \times \rho_{CO2} \times E, \quad (2)$$

where M_{CO2} is the mass CO_2 storage capacity (Mt), A is the trap area (m^2), h is the thickness (m), ϕ is the porosity (lrb%), S_{iir} is the irreducible water saturation (lrb%), B is the formation volume factor (m^3/m^3), ρ_{CO2} is the density of CO_2 (k_g/m^3), and E is the coefficient of the capacity integrated by the traps, CO_2 sweep, and buoyancy efficiency (IEA 2020; Anon 1981).

The CO_2 storage mass can be characterized as an effective capacity by multiplying by the storage effective coefficient, C, which is the trapping efficiency. The storage mass can be determined based on the reservoir simulation. The trap area, thickness, and porosity were precisely estimated using the 3-D reservoir geological model. Therefore, rather than Eq. (2), we changed the grid pore summation volumes $\left(V_{PV} = \sum_i A_i \times h_i \times \phi_i\right)$ to replace $A \times h \times \phi$, where A_i is the grid area, h_i is the grid thickness, and ϕ_i is the porosity of the grid; thus, the new equation was as follows (Vo Thanh et al. 2019):

$$M_{CO2} = V_{PV} \times \left(1 - S_{wiir}\right) \times B \times \rho_{CO2} \times E, \quad (3)$$

where V_{PV} is the total pore volume (m^3).

Results and discussion

3-D reservoir geological models

In block Nv32 of the Shenvsi oilfield, the Es1 Formation was the main reservoir rock, which was divided into four zones, i.e., Es1×1, Es1×2, Es1×3, and Es1×4, from top to bottom, based on the well log and seismic data, providing effective compatibility (Figs. 5 and 6). The geological characteristics, such as the significant change in thickness of the four Es1 zones, were obtained based on the correlations of the wells used in this study (Fig. 5f). The four horizons were also mapped in 3-D model space. These reservoir units are laterally extensive throughout the model area and influenced by the interpreted normal faults (Fig. 5a–d).

The seismic data, horizon, and fault surfaces were interpreted (Fig. 6a–c), followed by structural modeling (Fig. 6e). The structural model of block Nv32 displays a network of faults related to the syndepositional tectonic event. These sets of normal faults control the entire area of block Nv32, covering up to 70%; they are mainly NE–SW-trending and dip toward the NW–SE (Fig. 6d).

The petrophysical models of block Nv32 were developed based on the petrophysical parameters, i.e., porosity, permeability, and net-to-gross ratio (NTG). These were obtained through a well log analysis of the wells (Fig. 1).

Porosity refers to the quantity of oil that occupies the pore space of a reservoir. Thus, the oil volume capacity in the oil reservoir was estimated by measuring its porosity.

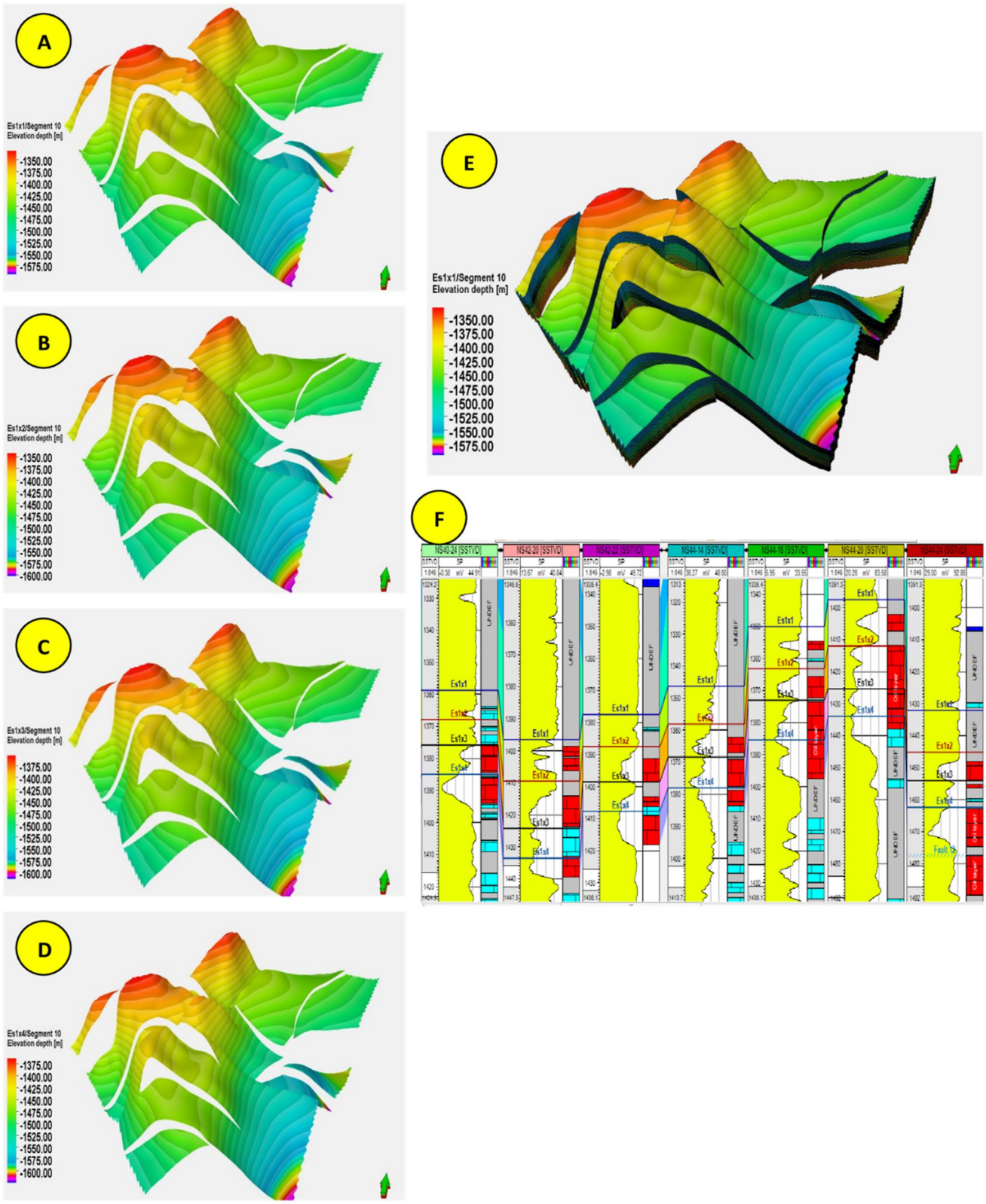

Fig. 5 Results of surface modeling in block Nv32. Elevation depths (m) of the **a**. Es1 × 1, **b**. Es1 × 2, **c**. Es1 × 3, and **d**. Es1 × 4 reservoir units. E. Depth modeling of all of the Es1 reservoir units. F. Cross section of the wells used in this study

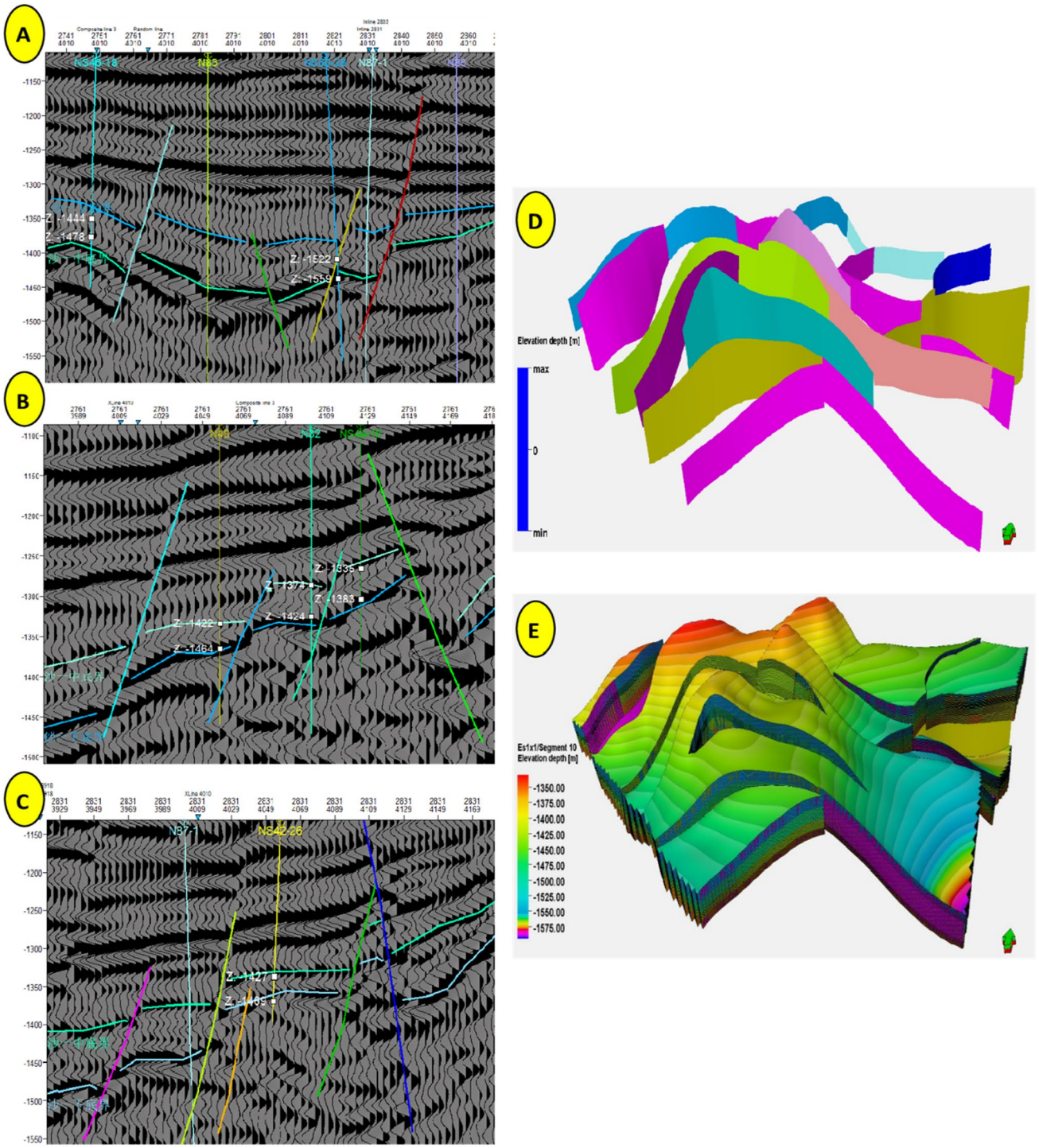

Fig. 6 Structural modeling results for block Nv32. The left panel presents the seismic sections **a**–**c** showing the reservoir tops of the Es1 Formation associated with normal faults. **d**. Surfaces of the fault network in the NE–SW, NW–SE, and E directions. **e**. Structural modeling presenting the depths of the Es1 reservoir units in contact with the normal faults

Permeability is another crucial parameter for determining the characteristics of reservoir rocks. Permeability is utilized to facilitate the transmission of reservoir fluid in the subsurface rock to the well surface.

Fig. 7 Results of the reservoir porosity modeling for block Nv32. The ▶ left panel presents the porosity maps of the **a**. Es1×1, **b**. Es1×2, **c**. Es1×3, and **d**. Es1×4 reservoir units. **e**. Porosity modeling of all of the ES1 reservoir units. F. Cross-sectional porosity model of the wells used in this study

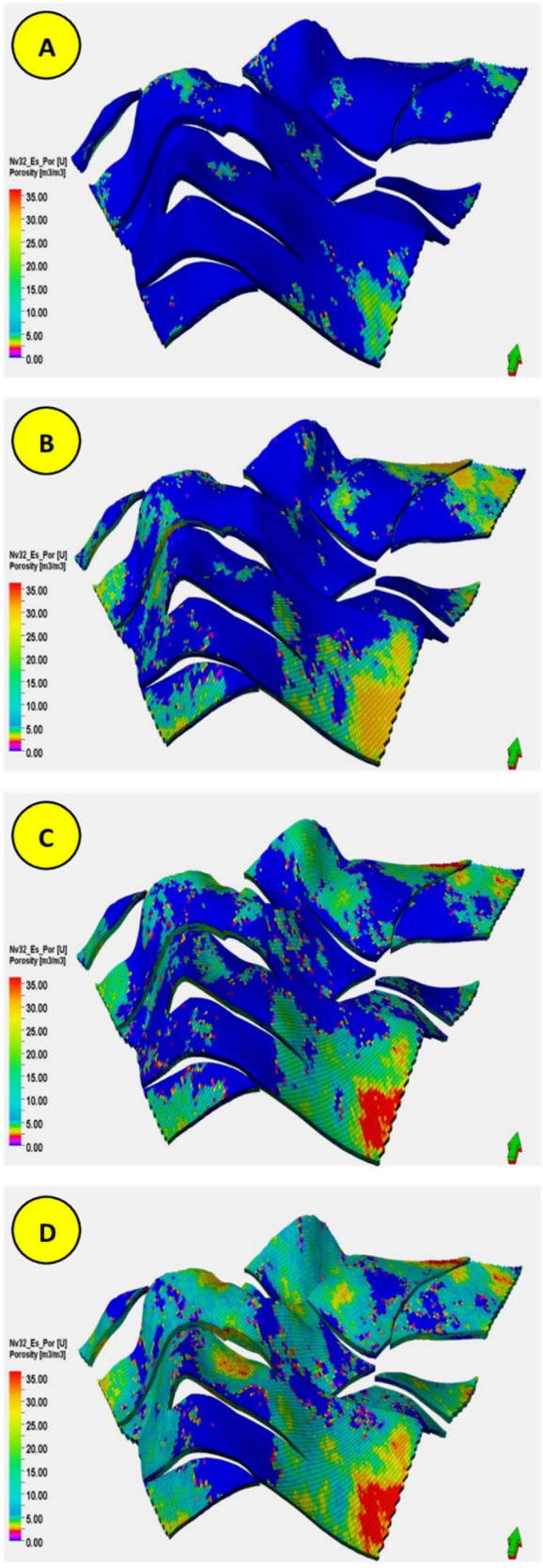
A
B
C
D
Nv32_Es_Por [U]
Porosity [m3/m3]
35.00
30.00
25.00
20.00
15.00
10.00
5.00
0.00

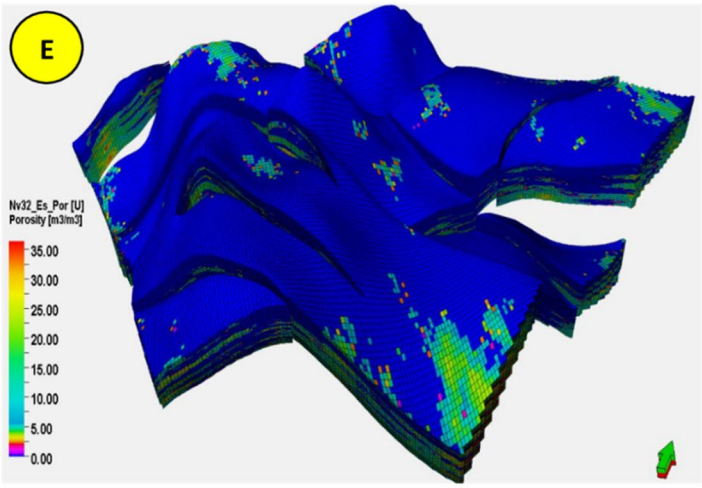
E
Nv32_Es_Por [U]
Porosity [m3/m3]
35.00
30.00
25.00
20.00
15.00
10.00
5.00
0.00

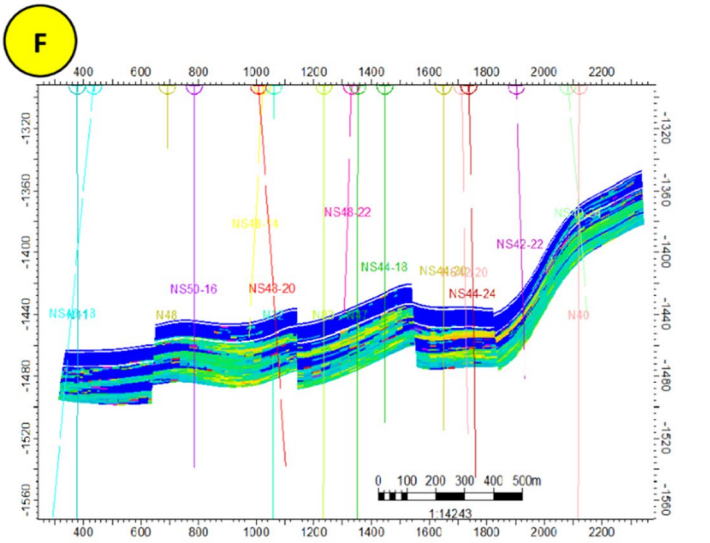
F
400
600
800
1000
1200
1400
1600
1800
2000
2200
-1320
-1360
-1400
-1440
-1480
-1520
-1560
NS48-22
NS42-22
NS44-18
NS50-16
NS48-20
NS44-24
N48
N40
0 100 200 300 400 500m
1:14243

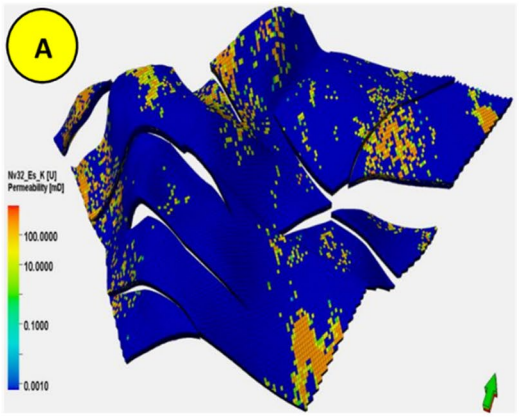
A
Nv32_Es_K [U]
Permeability [mD]
100.0000
10.0000
0.1000
0.0010

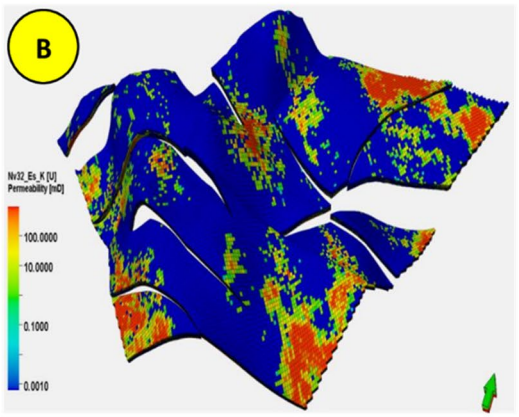
B
Nv32_Es_K [U]
Permeability [mD]
100.0000
10.0000
0.1000
0.0010

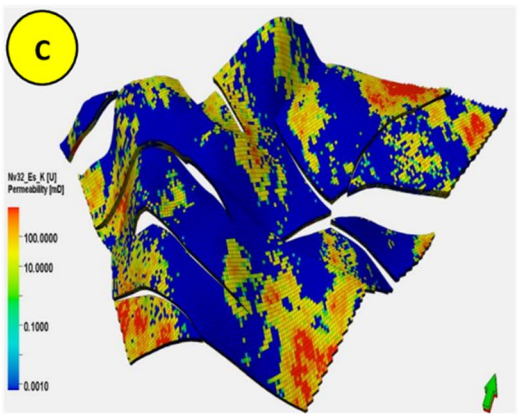
C
Nv32_Es_K [U]
Permeability [mD]
100.0000
10.0000
0.1000
0.0010

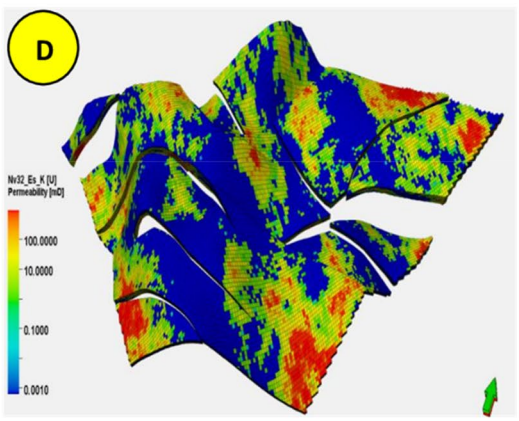
D
Nv32_Es_K [U]
Permeability [mD]
100.0000
10.0000
0.1000
0.0010

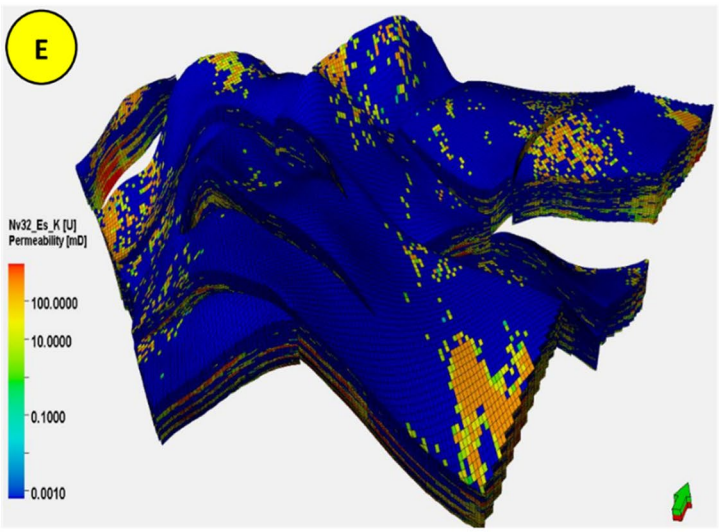
E
Nv32_Es_K [U]
Permeability [mD]
100.0000
10.0000
0.1000
0.0010

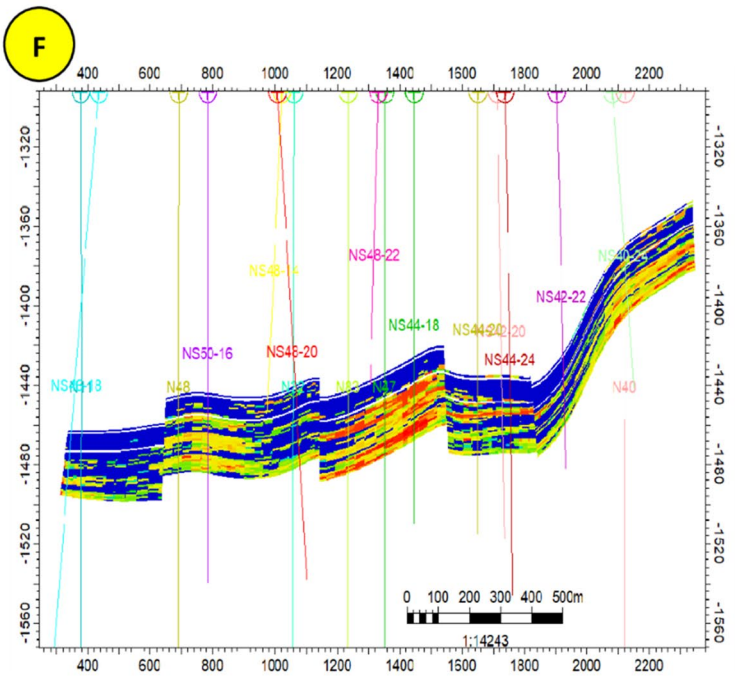
F
400
600
800
1000
1200
1400
1500
1800
2000
2200
-1320
-1360
-1400
-1440
-1480
-1520
-1560
NS48-22
NS42-22
NS44-18
NS50-16
NS48-20
NS44-24
N40
0 100 200 300 400 500m
1:14243

◂**Fig. 8** Results of the reservoir permeability modeling for block Nv32. The left panel presents the permeability maps of the **a**. Es1 × 1, **b**. Es1 × 2, **c**. Es1 × 3, and **d**. Es1 × 4 reservoir units. **e**. Permeability modeling of all of the ES1 reservoir units. F. Cross-sectional permeability model of the wells used in this study

In this study, the petrophysical investigation identified four principal reservoir intervals, i.e., Es1 × 1, Es1 × 2, Es1 × 3, and Es1 × 4, from the top to the bottom. These reservoir units have average porosity and permeability values ranging from 2 to 36% and 0.017–974.8 mD, respectively. In contrast, the NTG ratios of these reservoir units have relatively low to high values ranging from 0.60 to 1.00. These petrophysical results were mapped and dispersed in a 3-D model space by up-scaling the assigned values and understanding the reservoir quality within block Nv32.

Petrophysical models, including the porosity, permeability, and NTG ratio, were built for each reservoir unit throughout block Nv32 by employing the SGS technique. The 3-D models indicate that the petrophysical parameters of these four reservoir units extend laterally within the block Nv32 model, influenced by the interpreted normal faults. However, these models facilitated simulations of the spatial distribution of the petrophysical parameters and were used to determine the volume (STOIIP) of the reservoir units, indicating potential locations for future evolution within the oilfield. The 3-D spatial distribution indicates the presence of high porosity and permeability in the Es1 × 2, Es1 × 3, and Es1 × 4 reservoir units, as shown by the yellow–red color range (Figs. 7B–D and 8B–D).

In contrast, models for the Es1 × 1 reservoir unit exhibited lower porosity and permeability values (based on the blue–green color scheme in Figs. 7A and 8A). We note that the interpreted lithofacies of these units affect the principal petrophysical parameters of the reservoir units. In summary, the 3-D facies model revealed that the Es1 Formation is, in terms of the lithology, a more heterogeneous reservoir rock, showing a generally larger probability distribution of shale (dominantly) and sandstone, with minor limestone, both vertically and laterally (Fig. 9).

The presence of low porosity and permeability values within the Es1 × 1 reservoir unit can likely be attributed to the presence of high shale lithofacies (Fig. 9A) because shales are commonly characterized by low petrophysical properties, i.e., porosity and permeability.

The NTG models of the Es1 × 1, Es1 × 2, Es1 × 3 and Es1 × 4 units were also mapped in a 3-D model space based on the validity of the 3-D porosity and permeability models. The NTG model agreed with the 3-D reservoir property models for the porosity and permeability, revealing that the Es1 × 2, Es1 × 3, and Es1 × 4 reservoir units generally have good NTG ratio values between 0.60 and 1.00, as indicated by the green to red colors in Fig. 10B–D. Moreover, the structural limbs of the Es1 × 1 unit in the model had significant NTG ratio values (Fig. 10A).

STOIIP Determination

The reservoir volume (STOIIP) was the last stage for assessing the oil capacity in the reservoir, which aimed to estimate the quantity of HCs in the reservoir (El Khadragy et al. 2017). Reservoir characteristics, including the porosity, permeability, and NTG ratio, are commonly used as input data to determine the reservoir volume (Edwards and Santogrossi 1989).

The modeled petrophysical parameters of the Es1 reservoir units, including the porosity, permeability, and NTG ratio (Figs. 7, 8, and 10), were utilized to determine the reserves in accordance with the STOIIP of block Nv32. The STOIIP of block Nv32 was estimated at approximately 20.0819×10^6 sm^3.

The 3-D spatial distribution indicated the presence of high potential reserves in the Es1 × 2, Es1 × 3, and Es1 × 4 reservoir units, with volumes (STOIIP) of 4.70694, 4.78284, and 10.03771×10^6 sm^3, respectively (Fig. 11). These reservoir units have porosities, permeabilities, and NTG ratios of 2–36%, 0.017–974.8 mD, and 0.60–1.00, respectively (Figs. 7b–d, 8b–d, and 10b–d). In contrast, the petrophysical property models showed that the porosity, permeability, and NTG ratio of the Es1 × 1 reservoir unit in block Nv32 are 2–15%, 0.017–100 mD, and 0.10–0.25, respectively (Figs. 7a, 8a, and 10a). Moreover, we estimated a volume (STOIIP) of 0.554368×10^6 sm^3 (Fig. 11).

Geological uncertainties in the petrophysical models

Spatial uncertainties refer to reservoir properties that differ spatially, including the petrophysical properties ratio

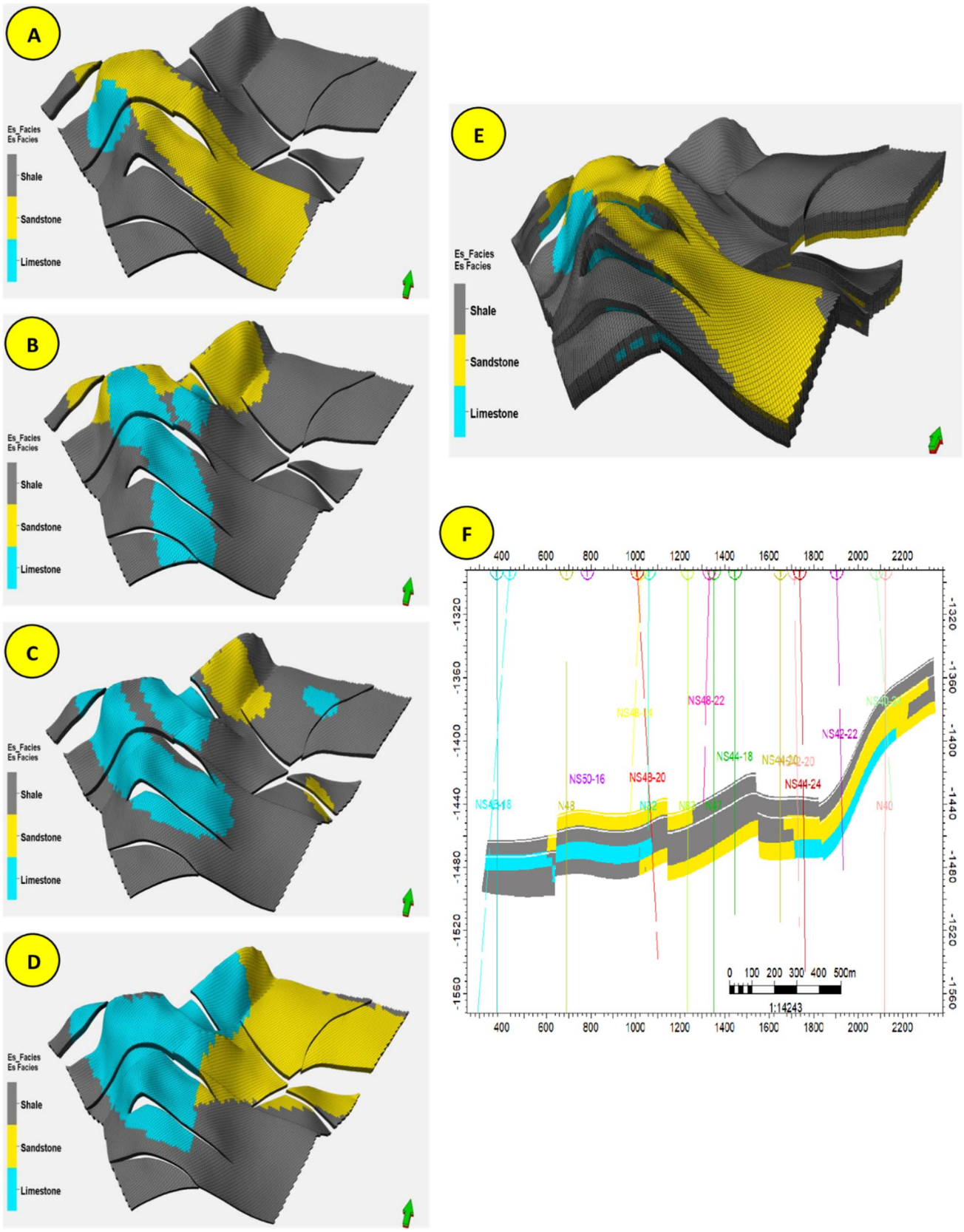

Fig. 9 Facies modeling results for block Nv32. The left panel presents the facies maps of the **a**. Es1×1, **b**. Es1×2, **c**. Es1×3, and **d**. Es1×4 reservoir units. **e**. Facies modeling of all of the ES1 reservoir units. **f**. Cross-sectional facies model of the wells used in this study

(Almeida et al. 2020). Sites for CO_2 sequestration typically contain significant uncertainty within their geological characteristics, including the uncertainty in the petrophysical properties (Chen et al. 2020; Jin et al. 2020; Heath et al. 2012). Structural interpretation is typically achieved using many assumptions, which leads to more uncertainties in the distribution of the reservoir properties in the structural models. Additionally, the core and well log data represent the porosity and permeability, respectively. Therefore, geological uncertainties also occur in the petrophysical models. Consequently, the models utilized for reservoir forecasting are vulnerable to various forms of uncertainty; moreover, interpreting and quantifying uncertainty is the most challenging aspect of modeling (Demyanov et al. 2019). Therefore, we considered the geostatistical parameters for the geological uncertainties. These parameters included the major, minor, and vertical directions, with values between 600 and 800 (base value of 600), 400–700 (base value of 500), and 2–50 (base value of 10), respectively. Table 1 lists the geostatistical parameters for the geological uncertainty. These geostatistical parameters generated a large number of operations with respect to the geological uncertainties. However, computing the pore volume is essential for determining the geological uncertainty. Therefore, 100−400 operations were conducted for the geological uncertainty, which was used to estimate the pore volume by altering the variogram parameters in the Petrel software (Fig. 12). The Monte Carlo sampling approach was employed to compute the probability distribution of the pore volume.

Figure 12 presents the geological uncertainty for the theoretical CO_2 storage capacity in block Nv32, Shenvsi oilfield. This figure demonstrates the idea of the selected number of realizations, which will vary from case to case. The P10, P50, and P90 statistics were adopted for the risk evaluation of the theoretical CO_2 storage capacity, which shows that an increase in the number of operations up to 400 does not change the results when compared with the use of 200 realizations. However, the results of the pore volume uncertainties were similar to those of the uncertainty assessment based on 200 geological operations. Therefore, 200 was deemed the optimal number of realizations for the CO_2 storage evaluation. Table 2 presents the computed pore volumes using the P10, P50, and P90 statistics using geological realizations.

Theoretical CO_2 storage capacity

Estimating the CO_2 storage capacity in a tight oil formation is convenient and straightforward, as compared with coal bed methane (CBM) and deep saline aquifers (DSA). Furthermore, petroleum reservoirs are better known and characterized than CBM and DSA media. Moreover, petroleum reservoirs are discrete instead of continuous, which allows for CO_2 storage in petroleum reservoirs. The total capacity of all the reservoirs in an area determines the CO_2 storage capacity in the petroleum reservoirs of a specific area and at a given scale, computed based on the reservoir properties, including the oil initial in place (OIIP), temperature (T), pressure (P), permeability (k), and porosity (ϕ). The Carbon Sequestration Leadership Forum introduced a set of approaches to estimate the CO_2 storage capacity for structural and stratigraphic trapping, dissolution trapping, and residual gas saturation trapping. Based on these guidelines, the theoretical CO_2 storage capacity was computed using Eq. (3). The least likely, P10, storage capacity was 15.6 million tons, whereas the most likely, P90, storage capacity was 207.9 million tons. Therefore, this tight oil reservoir has the potential for CO_2 storage, as indicated by the large quantity of CO_2. Although this unconventional oil reservoir poses challenges for CO_2 injection, the carbon capture utilization and storage guidelines suggest that a tight oil formation is a promising CO_2 injection site. The advantage of tight oil reservoirs for CCUS includes improved oil recovery and a decrease in the rate of CO_2 emissions. Additionally, the capability of these formations is unknown in the CCUS community. Thus, the theoretical CO_2 storage capacity was evaluated to determine the potential of a tight oil reservoir. In summary, the advantage of CO_2-EOR in tight oil reservoirs is the possibility of an additional storage site in the CCUS network. Owing to data availability limitations, which hinder our understanding of the CO_2 flows in tight oil reservoirs, the result of this study provide a preliminary indicator for the CCUS in unconventional oil-bearing formations. Furthermore, we plan to develop

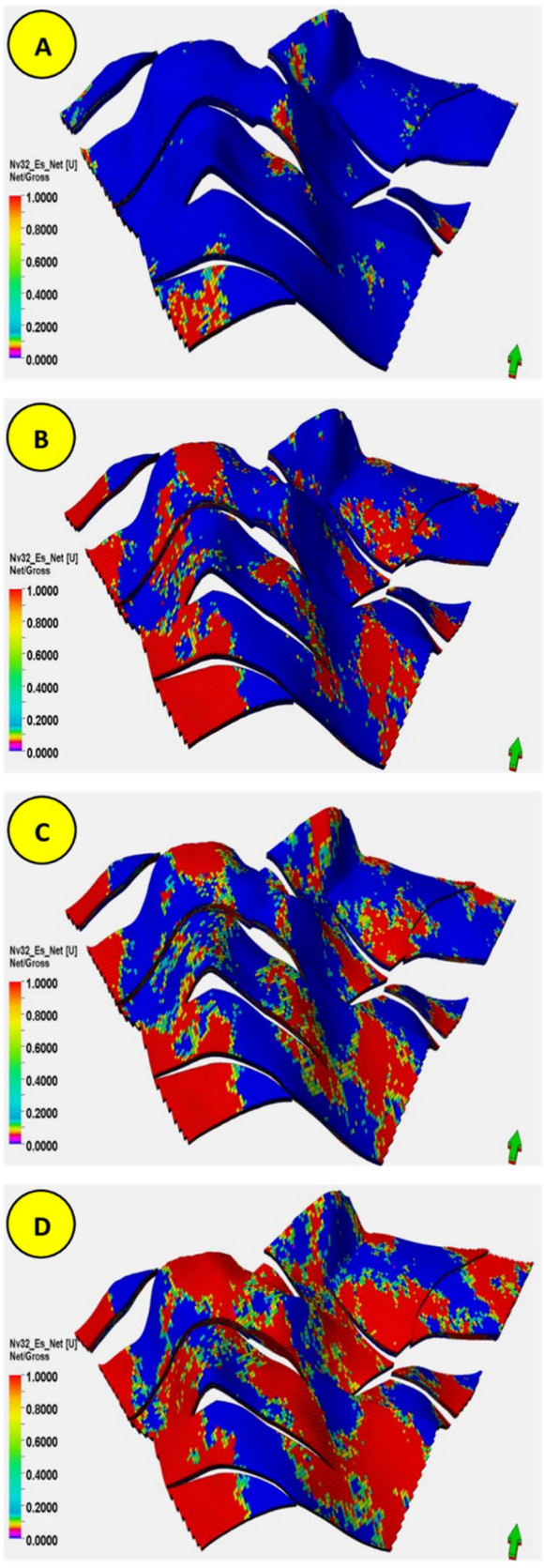
A
B
C
D
E
F
Nv32_Es_Net [U]
Net/Gross
1.0000
0.8000
0.6000
0.4000
0.2000
0.0000
NS48-14
NS48-22
NS42-22
NS44-18
NS44-20
NS50-16
NS48-20
NS44-24
N40
0 100 200 300 400 500m
1:14243

◂**Fig. 10** Results of the net-to-gross (NTG) ratio modeling for block Nv32. The left panel presents the NTG maps of the **a**. Es1×1, **b**. Es1×2, **c**. Es1×3, and **d**. Es1×4 reservoir units. **e**. NTG modeling of all of the ES1 reservoir units. **f**. Cross-sectional NTG model of the wells used in this study

Table 1 Geostatistical parameters for the geological uncertainties

Parameters	Min	Base value	Max
Major direction	600	600	800
Minor direction	400	500	700
Vertical	2	10	50

a dynamic reservoir model for CO_2 injection in unconventional oil reservoirs. Further data collection will be conducted to evaluate the compositional CO_2 interaction in the reservoir. Table 3 lists the theoretical CO_2 storage capacity for P10, P50, and P90 in block Nv32.

Summary and conclusion

We performed a comprehensive study on integrated 3-D geological reservoir models under geological uncertainty in the Es1 Formation in block Nv32, Shenvsi oilfield, with a multi-objective function to improve oil recovery and estimate the CO_2 storage capacity. The main conclusions obtained from this study are summarized below.

- The seismic and well log data indicate that the Es1 formation can be divided into four reservoir units. Shale is the dominant lithology, with intercalations of sandstone and limestone shale within the reservoir units, affected by interpreted normal faults.
- The well log data also indicate that the Es1×2, Es1×3, and Es1×4 reservoir units generally exhibit 2–36% porosity, 0.017−974.8 mD permeability, and moderate to good NTG ratios, i.e., good reservoir quality.
- The reservoir geological models show that there are lateral heterogeneities in the petrophysical properties and lithofacies of the reservoir.
- The reservoir geological models were employed to calculate the reservoir volume of the units in the Shahejie Formation of block Nv32. The four reservoir units in the Es1 Formation have volumetric values between 0.554368×10^6 and 10.03771×10^6 sm^3, with a total volumetric value of 20.0819×10^6 sm^3.
- According to the results of the uncertainty analysis for the geological model, 100–400 realizations were used in the uncertainty evaluation to estimate the pore volume. The results indicate that the appropriate number of realizations is 200. This number of geological realizations were reduced the uncertainties in the 3D model.
- The results for the theoretical CO_2 storage capacity indicate that the least likely, P10, range capacity was 15.6 million tons, whereas the most likely, P90, storage capacity was 207.9 million. A large CO_2 storage capacity demonstrates that tight oil formations may be a new sink for CCUS researchers.
- The results of the model indicate that the ES1 formation in block Nv32 has a combined potential for CO_2 storage and EOR.

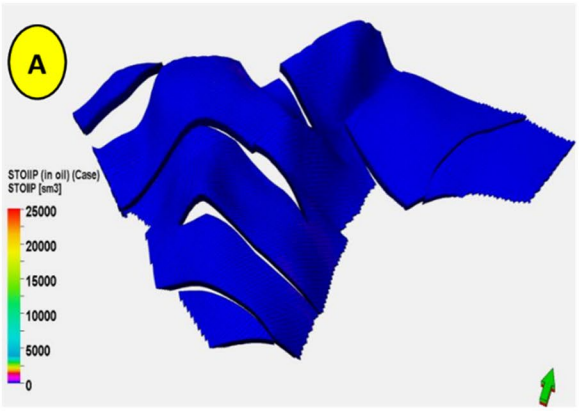

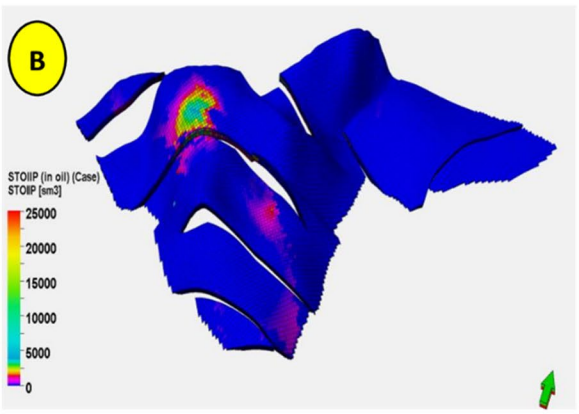

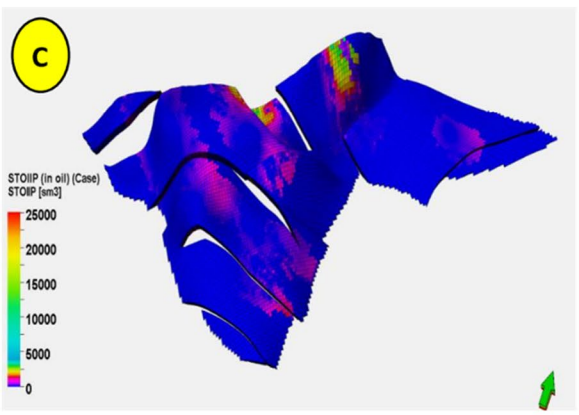

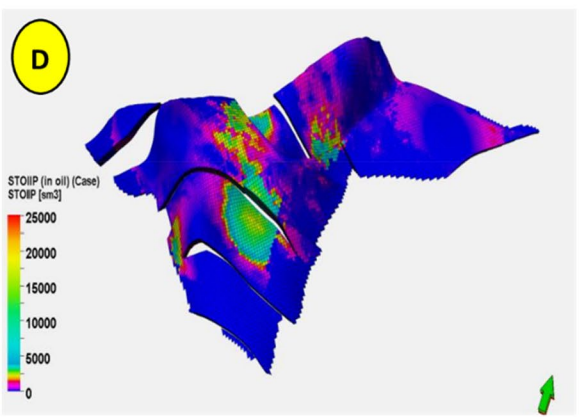

E

Zones	Bulk volume [x10^{6}m^3]	STOIIP (in oil) [x10^6 sm^3]
Es1x1	43.894771	0.554368
Es1x2	36.879991	4.7069397
Es1x3	29.936135	4.7828403
Es1x4	27.843010	10.0377143
Case	138.553907	20.0819

◂**Fig. 11** Modeling results for the volume (STOIIP) estimation in block Nv32. The left panel presents the estimated STOIIP of the **a**. Es1×1, **b**. Es1×2, **c**. Es1×3, and **d**. Es1×4 reservoir units. **e**. Table presenting the total estimated STOIIP and bulk volume values for all of the Es1 reservoir rocks

- Future studies should attempt to enhance our understanding of the CO_2 storage potential in tight oil formations. The field production history should be first updated in the history-matching reservoir models.

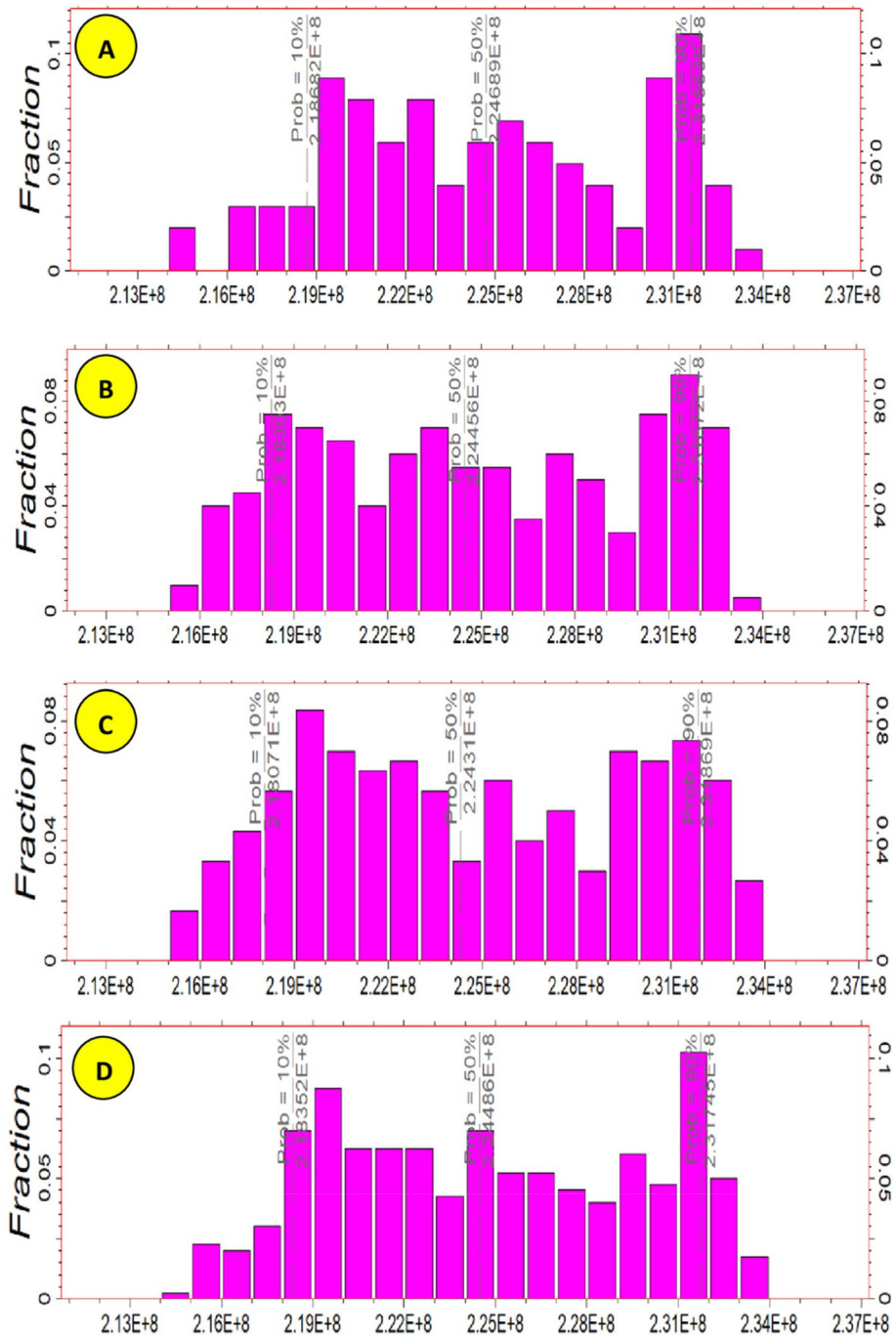

Fig. 12 Geological uncertainty associated with the theoretical CO_2 storage capacity of block Nv32, Shenvsi oilfield. The left panel presents the pore volume histograms based on **a**. 100, **b**. 200, **c**. 300, and **d**. 400 realizations

Table 2 Computed pore volumes using the P10, P50, and P90

Probability	100 Realizations	200 Realizations	300 Realizations	400 Realizations
P10	218.6 m3	218.3	218.1	218.3
P50	224.6 m3	224.4	224.3	224.4
P90	231.5 m3	231.7	231.8	231.7

Table 3 Theoretical CO_2 storage capacity for P10, P50, and P90

Parameters	Symbol	Unit	P10	P50	P90
Total pore volume	V_{PV}	Mm^3	218.3	224.6	231.5
Irreducible water saturation	S_{wiir}	%	0.36	0.26	0.11
Formation volume factor	B	Bbl/STB	1.46	1.46	1.46
Average CO_2 density	ρ_{CO2}	ton/m^3	0.768	0.768	0.768
Capacity coefficient	E	%	0.1	0.5	0.9
CO_2 storage capacity	M_{CO2}	Mt	15.66563	93.18061	207.9206

History-matching models can represent the reliability of future dynamic reservoir simulations. Second, rock–fluid interactions must be analyzed to understand information on the relative permeability in the dynamic reservoir models.

Funding No funding was received for conducting this study.

Declarations

Conflict of interest The authors declare no conflicts of interest.

References

Abdel-Fattah MI, Metwalli FI, Mesilhi ESI (2018) Static reservoir modeling of the Bahariya reservoirs for the oilfields development in South Umbarka area, Western Desert. Egypt J Afr Earth Sci 138:1–13. https://doi.org/10.1016/j.jafrearsci.2017.11.002

Abdideh M, Bargahi D (2012) Designing a 3D model for the prediction of the top of formation in oil fields using geostatistical methods. Geocarto Int 27:569–579. https://doi.org/10.1080/10106049.2012.662529

Agyare Godwill P, Waburoko J (2016) Application of 3D reservoir modeling on Zao 21 oil block of Zilaitun oil field. J Petrol Environ Biotechnol 07:1–8. https://doi.org/10.4172/2157-7463.1000262

Alcalde J, Flude S, Wilkinson M et al (2018) Estimating geological CO_2 storage security to deliver on climate mitigation. Nat Commun 9:2201. https://doi.org/10.1038/s41467-018-04423-1

Almeida F, Davolio A, Schiozer DJ (2020) Reducing uncertainties of reservoir properties in an automatized process coupled with geological modeling considering scalar and spatial uncertain attributes. J Petrol Sci Eng. https://doi.org/10.1016/j.petrol.2020.106993

Al-Mudhafar WJ (2018) How is multiple-point geostatistics of lithofacies modeling assisting for fast history matching? A case study from a sand-rich fluvial depositional environment of Zubair formation in South Rumaila oil field. Proc Annu Offshore Technol Conf 2:1485–1512. https://doi.org/10.4043/28662-ms

Ampomah W, Balch R, Will R et al (2017a) Co-optimization of CO_2-EOR and storage processes under geological uncertainty. Energy Procedia 114:6928–6941. https://doi.org/10.1016/j.egypro.2017.03.1835

Ampomah W, Balch RS, Cather M et al (2017b) Optimum design of CO_2 storage and oil recovery under geological uncertainty. Appl Energy 195:80–92. https://doi.org/10.1016/j.apenergy.2017.03.017

Anderson ST (2017) Cost implications of uncertainty in CO_2 storage resource estimates: a review. Nat Resour Res 26:137–159. https://doi.org/10.1007/s11053-016-9310-7

Anon (1981) World energy outlook

Bradshaw J, Bachu S, Bonijoly D et al (2007) CO_2 storage capacity estimation: issues and development of standards. Int J Greenhouse Gas Control 1:62–68. https://doi.org/10.1016/S1750-5836(07)00027-8

Bueno JF, Drummond RD, Vidal AC, Sancevero SS (2011) Constraining uncertainty in volumetric estimation: a case study from Namorado Field, Brazil. J Petrol Sci Eng 77:200–208

Chen B, Harp DR, Lu Z, Pawar RJ (2020) Reducing uncertainty in geologic CO_2 sequestration risk assessment by assimilating monitoring data. Int J Greenh Gas Control. https://doi.org/10.1016/j.ijggc.2019.102926

Dai Z, Viswanathan H, Middleton R et al (2016) CO_2 accounting and risk analysis for CO_2 sequestration at enhanced oil recovery sites. Environ Sci Technol 50:7546–7554. https://doi.org/10.1021/acs.est.6b01744

Demyanov V, Arnold D, Rojas T, Christie M (2019) Uncertainty quantification in reservoir prediction: Part 2—Handling uncertainty in the geological scenario. Math Geosci 51:241–264. https://doi.org/10.1007/s11004-018-9755-9

Edwards JD, Santogrossi PA (1989) Divergent/passive margin basins. American Association of Petroleum Geologists, Tulsa

El Khadragy AA, Eysa EA, Hashim A, Abd El Kader A (2017) Reservoir characteristics and 3D static modelling of the Late Miocene Abu Madi Formation, onshore Nile Delta. Egypt J Afr Earth Sci 132:99–108. https://doi.org/10.1016/j.jafrearsci.2017.04.032

Heath JEE, Kobos PHH, Roach JDD et al (2012) Geologic heterogeneity and economic uncertainty of subsurface carbon dioxide storage. SPE Econ Manag 4:32–41. https://doi.org/10.2118/158241-PA

Hirsche K, Porter-Hirsche J, Mewhort L, Davis R (1997) The use and abuse of geostatistics. LEAD Edge 16:253–262. https://doi.org/10.1190/1.1437612

IEA (2020) Global energy review 2020. Glob Energy Rev. https://doi.org/10.1787/a60abbf2-en

Jika HT, Onuoha MK, Okeugo CG, Eze MO (2020) Application of sequential indicator simulation, sequential Gaussian simulation and flow zone indicator in reservoir-E modelling; Hatch Field Niger Delta Basin. Nigeria Arab J Geosci. https://doi.org/10.1007/s12517-020-05332-8

Jin X, Wang G, Tang P et al (2020) 3D geological modelling and uncertainty analysis for 3D targeting in Shanggong gold deposit (China). J Geochem Explor. https://doi.org/10.1016/j.gexplo.2019.106442

Kamali MR, Omidvar A, Kazemzadeh E (2013) 3D geostatistical modeling and uncertainty analysis in a carbonate reservoir, SW Iran. J Geol Res 2013:1–7. https://doi.org/10.1155/2013/687947

Lelliott MR, Cave MR, Wealthall GP (2009) A structured approach to the measurement of uncertainty in 3D geological models. Q J Eng Geol Hydrogeol 42:95–105. https://doi.org/10.1144/1470-9236/07-081

Ling J, Qingkui W (2017) Application of sequence stratigraphy in depression lake in slope zone, taking Shenvsi oilfield as an example. IOSR JAGG 05:38–40. https://doi.org/10.9790/0990-0502013840

Mckee BN (2005) Technical group

Metwalli FI, Shendi EAH, Fagelnour MS (2017) Reservoir petrophysical modeling and risk analysis in reserve estimation; a case study from Qasr Field, north Western Desert, Egypt. IOSR JAGG 05:41–52. https://doi.org/10.9790/0990-0502014152

Pingping S, Xinwei L, Qiujie L (2009) Methodology for estimation of CO_2 storage capacity in reservoirs. Petrol Explor Dev 36:216–220. https://doi.org/10.1016/S1876-3804(09)60121-X

Pyrcz, Deutsch (2014) Book-geostatistical reservoir modeling Pyrcz and Deutsch

Rahim S, Li Z, Trivedi J (2015) Reservoir geological uncertainty reduction: an optimization-based method using multiple static measures. Math Geosci 47:373–396. https://doi.org/10.1007/s11004-014-9575-5

Rassas AAL, Ren S, Sun R et al (2020) Application of 3D reservoir geological model on Es1 formation, block Nv32, Shenvsi oilfield, China. OJOGas 05:54–72. https://doi.org/10.4236/ojogas.2020.52006

Satter A, Iqbal GM (2016) Determination of oil and gas in place: conventional and unconventional reservoirs

Spencer JC (1987) Environmental assessment strategies. Top Geriatr Rehabil 3:35–42. https://doi.org/10.1097/00013614-198710000-00007

Vo Thanh H, Sugai Y, Nguele R, Sasaki K (2019) Integrated workflow in 3D geological model construction for evaluation of CO_2 storage capacity of a fractured basement reservoir in Cuu Long Basin, Vietnam. Int J Greenh Gas Control. https://doi.org/10.1016/j.ijggc.2019.102826

Vo Thanh H, Sugai Y, Nguele R, Sasaki K (2020) Robust optimization of CO_2 sequestration through a water alternating gas process under geological uncertainties in Cuu Long Basin, Vietnam. J Nat Gas Sci Eng. https://doi.org/10.1016/j.jngse.2020.103208

Vo Thanh H, Sugai Y, Sasaki K (2020) Impact of a new geological modelling method on the enhancement of the CO_2 storage assessment of E sequence of Nam Vang field, offshore Vietnam. Energy Sources Part Recover Util Environ Eff 42:1499–1512. https://doi.org/10.1080/15567036.2019.1604865

Yin X, Lu S, Wang P et al (2017) A three-dimensional high-resolution reservoir model of the Eocene Shahejie Formation in Bohai Bay Basin, integrating stratigraphic forward modeling and geostatistics. Mar Petrol Geol 82:362–370. https://doi.org/10.1016/j.marpetgeo.2017.02.007

Zabalza-Mezghani I, Manceau E, Feraille M, Jourdan A (2004) Uncertainty management: from geological scenarios to production scheme optimization. J Petrol Sci Eng 44:11–25. https://doi.org/10.1016/j.petrol.2004.02.002

Zamora Valcarce G, Zapata T (2006) Three-dimensional structural modeling and its application for development of the El Portón field, Argentina, Ansa A, Selva G. Am Assoc Petrol Geol Bull 90:307–319. https://doi.org/10.1306/09300504142

Zhong Z, Carr TR (2019) Geostatistical 3D geological model construction to estimate the capacity of commercial scale injection and storage of CO_2 in Jacksonburg-Stringtown oil field, West Virginia, USA. . Int J Greenhouse Gas Control West Virginia Int J Greenh Gas Control 80:61–75. https://doi.org/10.1016/j.ijggc.2018.10.011